THERMODYNAMIC ANALYSIS OF A GAS OPERATED TRIPLE EFFECT ABSORPTION CYCLE

Md Azhar[1] and M. Altamush Siddiqui[2]

Asst. Prof., Department of Mechanical Engineering, Vivekananda College of Technology & Management, Aligarh,

India[1]

Professor, Department of Mechanical Engineering, Aligarh Muslim University, Aligarh, India[2]

Abstract: A Triple Effect Vapour Absorption cycle using LiBr-H_2O solution as working pair has been analysed and compared with the Single and Double Effect cycles. The sources of energy selected are liquefied petroleum gas (LPG) and compressed natural gas (CNG) because the triple effect system requires heat at relatively high temperature. The analysis is done for different values of the evaporator and the condenser temperatures; the absorber temperature is assumed to be equal to the main condenser temperature. The temperature and concentration of LiBr salt in the high pressure generator, to which heat is supplied, are varied simultaneously for fixed temperatures/pressures in the middle and high pressure condensers. Effect of the high pressure generator temperature on the coefficient of performance (COP), volume flow rate and cost of the LPG and CNG have been investigated.

Keywords: COP, LiBr-water, Triple Effect, LPG, CNG

I. INTRODUCTION

Vapour absorption cooling technology is one of the best alternatives to the vapour compression cooling system from the viewpoints of energy and environment. The attractive features that an absorption system possess are that it can operate using a low grade energy in the form of heat and uses natural substances as working fluids, which do not cause ozone depletion and global warming. Different combination of working fluids are possible for this system, the most common of them are H_2O-NH_3 and LiBr-H_2O. However, LiBr-H_2O system is simpler in design and operation, and also cheaper in cost as compared to the NH_3-H_2O system. The LiBr-H_2O mixture is used only in air-conditioning applications since water freezes at 0°C.

The world first triple effect gas absorption chiller was commercialized in October 5, 2005. This absorption chiller is a "green" air conditioning system that provides heating/ cooling for large commercial buildings. The triple effect chiller, in comparison to the double effect chillers, slashes energy consumption up to 30%. However, it requires high generator temperature to drive the system properly.

Saghiruddin and Siddiqui [1,2], Siddiqui [3], Malik and Siddiqui [4] performed thermodynamic and economic analysis of the single effect absorption cycle by using different working fluid [LiBr-H_2O, NH_3-H_2O , NH_3-$LiNO_3$ and NH_3-NaSCN] and different sources of energy [Biogas, LPG and Solar Collectors]. Aphornratana and Sriveerakul [5] carried experimental study on single effect absorption system using LiBr-H_2O. Kaushik and Kumar [6] performed thermodynamic study of two-stage vapour absorption refrigeration system using ammonia as refrigerant with liquid/solid absorbent. They used two combinations such as NH_3-H_2O and NH_3-$LiNO_3$. Arora and Kaushik [7] and Marcos et al. [8] performed energy and exergy analysis of single effect and double effect absorption LiBr-H_2O system. Gomri and Hakimi [9] performed energy and exergy analysis of double effect vapour absorption system and have shown that COP increases with increasing low pressure generator (LPG) temperature, but decreases with increasing high pressure generator (HPG) temperature. The analysis has been carried for fixed temperatures in the LPG and HPG. Gomri [10] investigated the potential for the application of single, double, triple effect absorption cooling cycles for the production of chilled water.

Gebreslassie et al. [11] carried first and second law analysis for half to triple effect water-LiBr absorption system. At higher heat source temperature, the COP and exergetic efficiency decreases slowly. Saeed and Hamid [12] carried out thermodynamic analysis of triple effect parallel flow absorption chiller for cooling and heating purposes and analysed coefficient of performance (COP) of the cycle. Their procedure of calculation is same as that of Gomri and Hakimi [9] and Gomri [10].

In most of the studies carried so far on the double and triple effect cycles, the calculations have been done for fixed temperatures in the generator, while concentration and pressure in them are varied for detailed analysis. However, in

the present study, the pressure in each generator is fixed. This subsequently fixes the refrigerant-saturation temperature in the condenser that corresponds to the pressure in the respective condenser-generator assembly. The salt concentration and temperature in each generator is then varied, which proceeds systematically and hence, simplifies the calculation. The studies have been carried for 1TR capacity of the triple effect system. Studies on the single and double effect cycles have also been conducted for the purpose of comparison. The analysis is done for the evaporator temperatures (T_e) of 5, 7.5, 10 and 12.5^{o}C and the main-condenser temperatures (T_c) of 30, 35 and 40°C. The secondary condenser temperature (T_{c2}) in the double and triple effect cycles are taken as: 80, 90 and 100°C, while in the high pressure condenser (T_{c1}) of the triple effect cycle are 150, 160 and 170°C.

II. SYSTEM DESCRIPTION

Figure 1 shows schematic diagram of Triple Effect vapour absorption system and its process on P-T-X diagram in Fig. 2. It consists of three generators: a high pressure generator (G), middle generator (G_M) and lower generator (G_L). It also consists of three condensers: a high pressure condenser (C_1), a secondary condenser (C_2) and main condenser (C) from which heat is rejected to the surrounding. The high pressure generator (G) and condenser (C_1) operate at high pressure, $P_4=P_g$. The Middle generator (G_M) and the secondary condenser (C_2) operate at pressure, $P_3=P_{gM}=P_{C2}$ while the lower generator (G_L) and main condenser operate at pressure, $P_2=P_{gL}=P_C$. The evaporator and the absorber work at low pressure ($P_1=P_e=P_a$). In this system, the weak solution at state 1 is pumped from the absorber to the high pressure generator (G_M) through three preheaters (i.e. PH1, PH2 and PH3). In the high pressure generator, solution is heated at relatively high temperature to boil out the refrigerant vapour from the solution. The vapour released from 'G' enters the high pressure condenser (C_1) and condenses. The heat of condensation at this condenser is utilized to heat the middle generator (G_M). The strong solution leaving the generator 'G' at state 10, flows into the generator 'G_M' through the preheater 'PH3', where solution is cooled to some extend by exchanging heat with the weak solution. In the generator 'G_M' some more vapour is released that enters the secondary condenser (C_2). The heat of condensation in C_2 is utilized to heat the lower generator (G_L). The stronger solution which is now leaving the generator 'G_M' at state 10c, then flows to the generator 'G_L' through 'PH2' where the solution is further cooled by exchanging heat with the weak solution. Thus, still more refrigerant is generated in 'G_L' that enters the main condenser 'C' from which heat is released to the sink. Thus, the total refrigerant entering the main condenser is the sum of all those coming from the three generators. The liquid-refrigerant from the condenser (C) flow into the evaporator through a precooler (PC) and a throttle valve which vaporizes after taking heat from the medium to be cooled. It then enters the absorber to be absorbed by the strongest solution coming from the lower generator (G_L) through the preheater PH1. The cycle then gets completed.
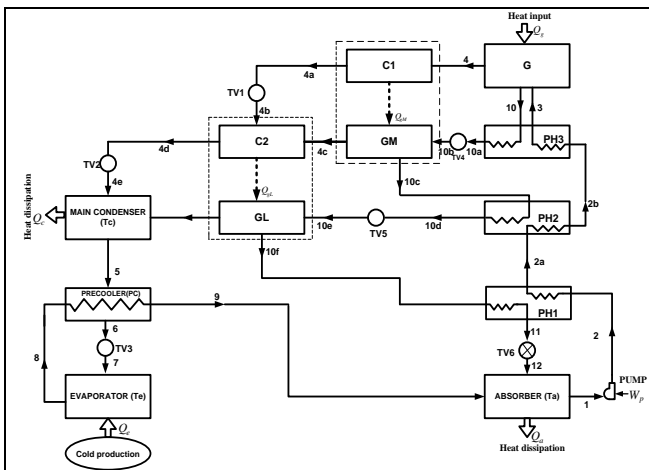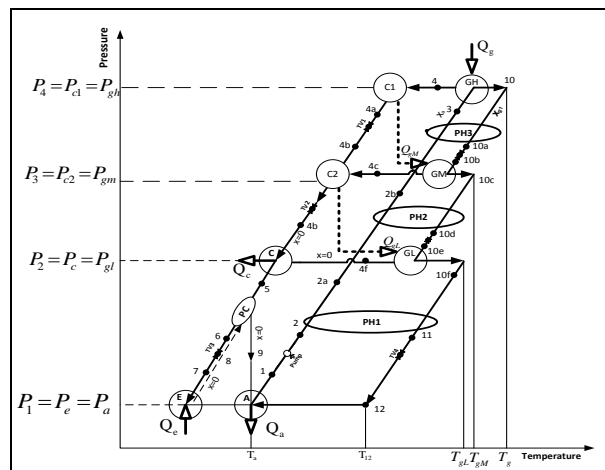

Fig.1 Triple Effect Absorption Refrigeration System

Fig.2 Triple Effect System on P-T-X diagram

For the single effect cycle, there will be no G_L, G_M, C_1, C_2, PH_1, PH_2, etc. In the Figs. 1 & 2, the state points will change as 2a=3, 10f=10 and the refrigerant at state 4 will enter the main condenser, C and leave it at state 5. Similarly, for the double effect cycle, there will be no G_L, C_2, PH_2. In the Figs. 1 & 2, the state points will change as 2a=2b, 10f=10c and the refrigerant at state 4b and 4c will enter the main condenser, C and leave it at state 5. The generator load $Q_{gM}=Q_{gs}$.

III. MATHEMATICAL MODELLING

A. ABSORPTION CYCLE

Assuming each component of system as control volume, energy balance lead to the following heat transfer equations:

Absorber: $\qquad\qquad\qquad\qquad\qquad Q_a = m_9 h_9 + m_{12} h_{12} - m_1 h_1$ $\qquad\qquad\qquad\qquad$ (1)

Solution pump: $\qquad\qquad\qquad\qquad W_p = m_2 h_2 - m_1 h_1$ $\qquad\qquad\qquad\qquad\qquad\quad$ (2)

Evaporator: $\qquad\qquad\qquad\qquad\quad Q_e = m_8 h_8 - m_7 h_7$ $\qquad\qquad\qquad\qquad\qquad\quad$ (3)

High pressure generator: $\qquad\qquad Q_g = m_4 h_4 + m_{10} h_{10} - m_3 h_3$ $\qquad\qquad\qquad\quad$ (4)

Condenser of the single effect cycle: $Q_c = m_4 h_4 - m_5 h_5$ $\qquad\qquad\qquad\qquad\qquad$ (5)

Secondary generator and main condenser of the double effect cycle: $Q_{gs} = m_{4c} h_{4c} + m_{10c} h_{10c} - m_{10b} h_{10b}$ $\qquad$ (6)

$\qquad\qquad\qquad\qquad\qquad Q_c = m_{4c} h_{4c} + m_{4b} h_{4b} - m_5 h_5$ $\qquad\qquad\qquad\qquad$ (7)

Middle and lower generators and main condenser of the triple effect cycle:

$$Q_{gM} = m_{4c} h_{4c} + m_{10c} h_{10c} - m_{10b} h_{10b} \qquad\qquad (8)$$

$$Q_{gL} = m_{4f} h_{4f} + m_{10f} h_{10f} - m_{10e} h_{10e} \qquad\qquad (9)$$

$$Q_c = m_{4e} h_{4e} + m_{4f} h_{4f} - m_5 h_5 \qquad\qquad (10)$$

(With neglecting pump work i.e. $W_p \approx 0$), $\quad COP = \dfrac{Q_e}{Q_g}$ $\qquad\qquad\qquad\qquad\qquad\qquad$ (11)

The crystallization limit in the system have been checked using the following equation, for $300 \leq T \geq 375$ K [13]:

$X_c = 9.8459E\text{-}02(T\text{-}273.15) + 59.7995$ $\qquad\qquad\qquad\qquad\qquad\qquad\qquad\qquad\qquad\quad$ (12)

B. SOURCE OF ENERGY

The absorption system can be driven by any source of heat energy such as solar, waste heat and gases. The triple effect system requires heat at relatively very high temperature (above 473.15 K). Since gases can burn at high temperature, therefore the sources of energy selected for heat input to these systems is gas. The liquefied petroleum gas (LPG) and compressed natural gas (CNG), that are easily available in the market, have been selected for the analysis. Both, LPG and CNG are less toxic greenhouse gases resulting in reduced pollution.

The liquefied petroleum gas is generally a mixture of number of gases such as propane, butane and ethane. For a typical composition of LPG, say Propane (C_3H_8) =6.88%, Iso-butane (C_4H_{10}) =16.54% and n-butane (C_4H_{10}) = 76.58%, average molecular weight of LPG comes out to be M= 57.0368 kg/kmole. The energy released as Absorption heat (Q_L) during combustion of LPG has been obtained by writing combustion equation for the above composition with 10% excess air, which is then calculated considering the respective values of enthalpy [14] at different temperatures of the products of combustion and correlated for the range of $273K \leq T_p \leq 1800K$ as:

$Q_L = 114272.75 - 39.5(T_p\text{-}273.5) - 5.4 \times 10^{-3} (T_p\text{-}273.15)^2$ kJ/m^3 $\qquad\qquad\qquad\qquad$ (13)

The specific volume of LPG will be: $\quad v = \dfrac{V}{M} = \dfrac{25.68}{57.036} = 0.4502 \text{ m}^3/kg$ $\qquad\qquad\qquad\qquad$ (14)

This states that at the atmospheric pressure, 1kg of LPG = 0.4502 m^3.

Similarly, for the Compressed natural gas (CNG), with composition as: methane, CH_4=91.9%, Ethane (C_2H_6) =3.7%, Propane (C_3H_8) = 1.2%, Iso butane (C_4H_{10})$_{iso}$= 0.4%, carbon dioxide (CO_2) = 2%, Nitrogen (N_2) = 0.2%, n-butane (C_4H_{10})$_n$ = 0.1% and Heptane (C_5H_{12}) = 0.4%, the average molecular weight comes out to be 17.857 kg/kmole.

And the energy released as heat (Q_C) during combustion of CNG, in the similar manner as for the LPG, is correlated for the range of $273K \leq T_p \leq 1800K$ as:

$Q_C = 36992.05 - 12.98(T_p\text{-}273.15) - 2.02 \times 10^{-3}(T_p\text{-}273.15)^2$ kJ/m^3 $\qquad\qquad\qquad\qquad$ (15)

The cost of gas is estimated in terms of capital and running costs. The capital cost will be that of its connection along with accessories. While the running cost of LPG will quantity of the gas used. The security money for commercial connections of LPG is Rs 2000, which includes the cylinder, regulator, pipes and burner costs. Therefore, the capital cost of LPG is fixed as: $\quad C_{1L}$= Rs 2000.00 $\qquad\qquad\qquad\qquad\qquad\qquad$ (16)

Since, running cost of LPG will be the cost of gas available for commercial connections at the rate of Rs. 1277/= per cylinder, therefore, the commercial LPG cylinder that contains 19 kg of gas (equivalent to 8.5538 m^3), will be of Rs. 149.29 per m^3. Thus, the running cost of LPG in one year will be: [Cost of gas per m^3 x volume flow rate of LPG (V_L in m^3/h) x 16 hours per day of operation of the absorption system x 325 days in a year]. This can be obtained as: C_{2L} = Rs. $[16 \times 325 \times 149.29 \times V_L]$ = Rs. 776308V_L $\qquad\qquad\qquad\qquad\qquad\qquad\qquad$ (17)

The CNG is filled in kits that are available in the market at various costs depending upon its quality. The Eco-Gas in Delhi, a government recognized company, sells a kit of 12 kg capacity at Rs.23000. The capital cost of CNG kit is therefore, fixed as: C_{1C} = Rs. 23000.0 (18)

The running cost of CNG will, however, be the cost of gas purchased from the gas-stations which is Rs. 38.34 per kg in New Delhi. Since 1 kg of CNG =1.4382 m^3 due to its specific volume, the cost of CNG per m^3 will be Rs. 26.658. Therefore, running cost of CNG in one year will be: [Cost of gas per m^3 x volume flow rate of CNG (V_C in m^3/h) x 16 hours per day of operation of the absorption system x 325 days in a year] . In a simple form it will be,

C_{2C} = Rs. $[16 \times 325 \times 26.658 \times V_C]$ = Rs. $138621.6 V_C$ (19)

The total cost of the gas, using present worth method spread over a period of 15 years, with 10% interest on the investment will come out to be,

$C_T = 6.667 \times 10^{-2} C_1 + 0.5778 C_2$ (20)

Where, V_L and V_C are volume flow rates of LPG and CNG, given below in terms of COP of the absorption system and heating value of the respective gas,

$$V_L = \frac{Q_g}{Q_L} = \frac{Q_e}{(COP \times Q_L)}, \quad m^3/h \tag{21}$$

$$V_C = \frac{Q_g}{Q_C} = \frac{Q_e}{(COP \times Q_C)}, \quad m^3/h \tag{22}$$

C. CALCULATION PROCEDURE

The thermodynamic properties of the refrigerant (water) and LiBr-H_2O mixture, such as specific enthalpy, specific heat, density, concentration, saturation pressure and temperature are calculated for each state point in the cycle using the available correlations [13,15-18] in the form of subroutines in a computer program. The analysis of the vapour absorption system is proceeded by taking the system cooling capacity as, 1 TR (Q_e =12600 kJ/h). In the triple effect cycle, heat is supplied to the high pressure generator. The middle generator operates by the heat rejected from the high pressure condenser, while the lower generator operates by using the heat rejected by the secondary condenser. The analysis has been done for the different values of temperature in the high pressure condenser, that is, $T_{c1}=150^oC$, etc. and temperature, $T_{c2}=80^oC$, etc. in the secondary condenser.

The concentration in the high pressure generator is assumed to be $X_{g1}=X_a+0.5$, and temperature in it (T_g) is calculated for the known values of T_{c1} and X_{g1}. Similarly, concentration in the middle generator is assumed as: $X_{g2}=X_{g1}+0.2$. Thus, knowing T_{c2} and X_{g2}, temperature in the middle generator (T_{g2}) is calculated. Now concentration of the lower, that is, the third generator is assume to be, $X_{g3}=X_{g2}+0.1$, and temperature in the lower generator corresponding to the X_{g3} and main condenser temperature T_c is calculated. This is continued with higher values of X_{g3}, iterating with finer values of X_{g3} until heat load of the lower generator (Q_{gL}) and secondary condenser (Q_{c2}) balance within an error of $\pm$ 0.1 kJ/h. This is repeated with increase in the value of X_{g2}. The temperature in the middle generator increases with increase in X_{g2}. This calculation proceeds with finer values of X_{g2} until heat load of the middle generator balances the heat rejected by the high pressure condenser. This is repeated with the increasing values of X_{g1} until the crystallization limit or till the balance of heat in the condenser and generator operating at two pressures is attained. Subsequently, the generator load, COP and volume/cost of the gases required, are evaluated for different values of T_e, $T_c=T_a$, T_{c1} and T_{c2}.

IV. RESULTS AND DISCUSSION

A. COEFFICIENT OF PERFORMANCE

Figure 3 shows variation in the coefficient of performance of the single, double and triple effect cycles with generator temperature (to which heat is supplied) at different values of the evaporator temperature. Here the main condenser temperature in single, double and triple effect cycles from which heat is rejected to the surrounding is $T_c=30^oC$. The secondary condenser temperature in the double and triple effect cycles is $T_{c2}=80$ and 100^oC, while in the triple effect cycle the high pressure condenser temperature is $T_{c1}=150^oC$ and 170^oC. From these plots it is seen that the coefficient of performance of the absorption cycle increase drastically from low values at the low generator temperatures, reach to a maximum value and then either remain constant with further increase in the generator temperature (as in the single effect cycle) or terminate (as in the triple effect cycle).
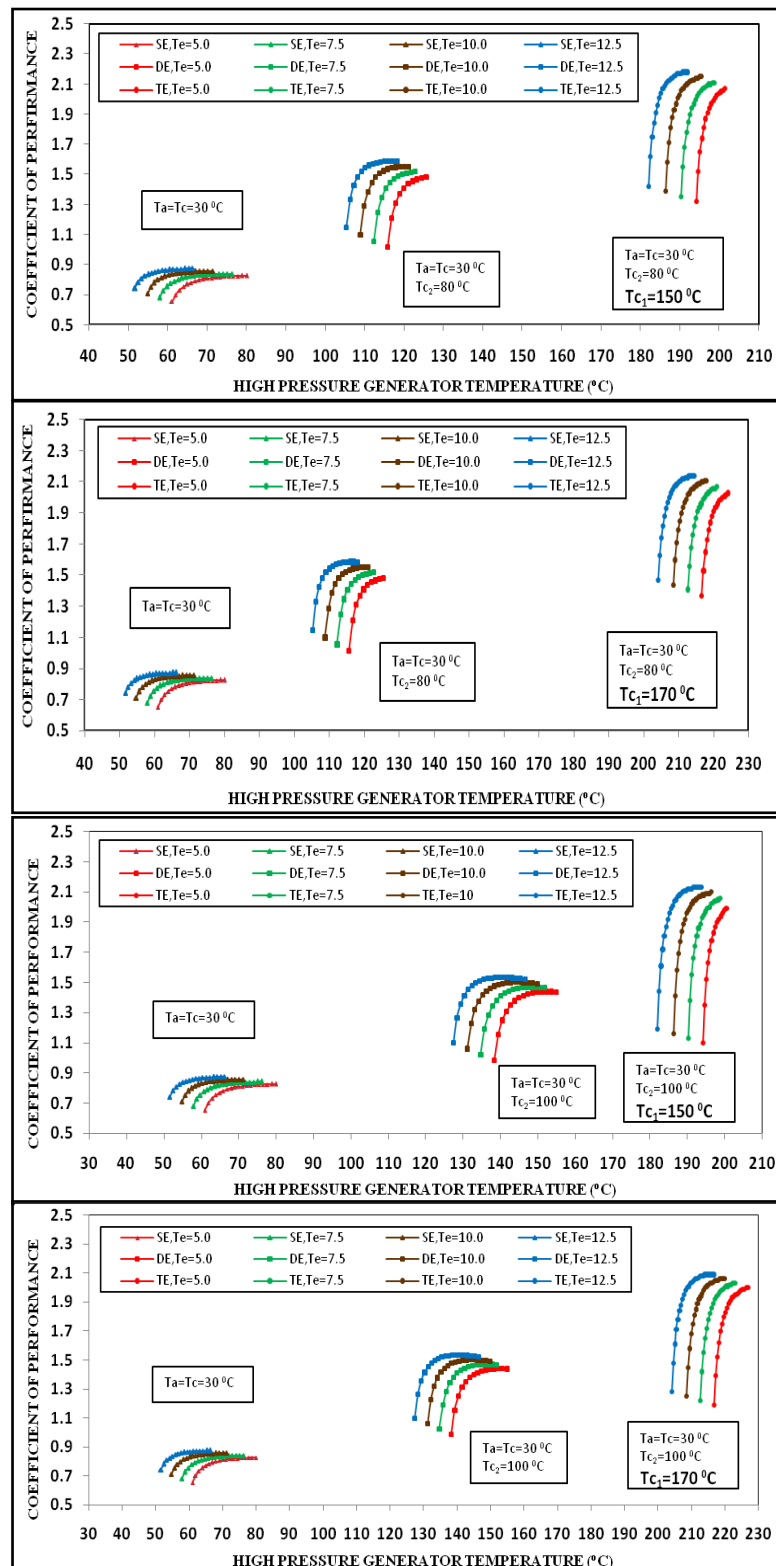
Fig. 3 Variation in COP of single, double and triple effect cycles with generator temperature (at $T_a=T_c=30^{\circ}C$, $T_{c2}=80$ &$100^{\circ}C$, $T_{c1}=150$ & $170^{\circ}C$).

This is because, in the single effect cycle there is no limit, other than crystallization, in increasing the generator temperature. While, in the double effect cycle, the generator temperature and concentration will terminate when heat rejected in the secondary condenser balances the heat input to the secondary generator; the constant values appear more at high T_{c2}. Similarly in the triple effect cycle, heat balance requirement at levels: between high pressure condenser and middle generator and, between medium pressure condenser and lower generator, again makes the generator temperature and concentration terminate relatively earlier than as it was observed in cases of the double and single

effect cycles. It is seen that with increase in the evaporator temperature, COP of all the cycles increase and shift towards low generator temperatures. One can also notice drastic increase in COP of the advance stage cycles, that is, $COP_{triple} > COP_{double} > COP_{single}$. Increase in temperature of any condenser whether it is at low, medium or high pressure, the COP of the absorption system generally decreases.

B. VOLUME FLOW RATES AND COST OF GASES

Figure 4 shows variation in the volume flow rates and total yearly cost of LPG and CNG for operating the single, double and triple effect cycles with generator temperature at different values of the evaporator temperature. It is observed that the volume flow rate of both gases in all the three cycles decrease on increasing the high pressure generator temperature, reach to minimum values and remain almost constant. Similar is the trend of the plots for the total yearly cost of both gases in all the three cycles.
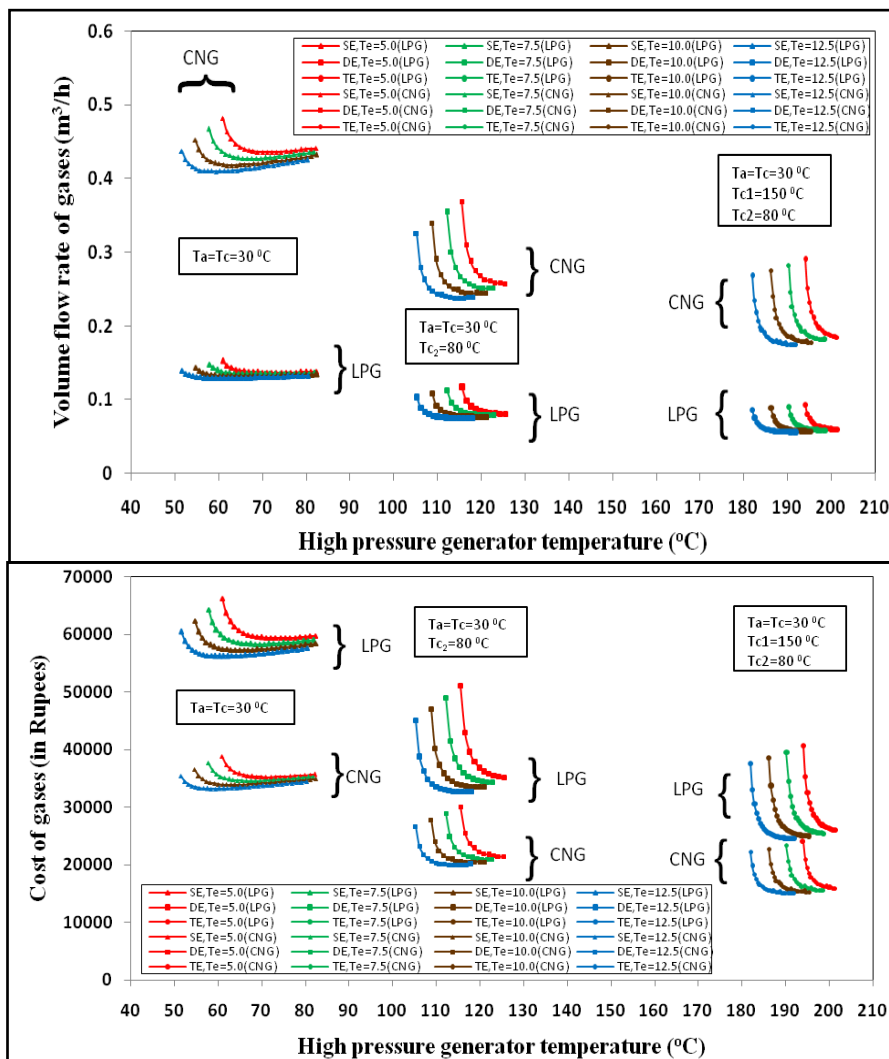

Fig.4 Variation in volume flow rates and yearly total cost of LPG and CNG with generator temperature at ($T_a=T_c=30$°C, $T_{c2}=80$°C and $T_{c1}=150$°C).

It is seen that the volume flow rate and total yearly cost of LPG and CNG gases decreases with increase in the evaporator temperature. The volume flow rate and cost of the gases decrease significantly in case of the double effect cycle from that of the single effect cycle, with still lower costs and volume flow rates in the triple effect cycle. It is also seen that the volume flow rate of CNG, V_c is greater than the flow rate of LPG, V_L in the single, double and triple effect cycles. This is because of difference in their specific volumes; the specific volume of CNG being greater than that of the LPG. However, the total cost of LPG is higher than CNG, because CNG is cheaper than LPG. It is found that, the volume flow rate and cost of both gases slightly increase with increase in temperatures of the secondary as well as the high pressure condensers.

V. CONCLUSIONS

a. Maximum COP of the single effect cycle comes out to be 0.7 to 0.86, that of the double effect cycle as1.2 to 1.55, while in the triple effect cycle it goes up to 2.16.

b. Increase in COP of the double effect cycle is 56 to 81% from that of the single effect cycle, and that of the triple effect is 103 to 152% higher than the single effect cycle.

c. The COP decreases with increase in the main condenser/absorber temperature and increases with rise in the evaporator temperature.

d. Operating cost of the double effect cycle is 57 to 68% of the single effect cycle and that of the triple effect cycle comes out to be 60 to 75% of those in the double effect and 40 to 45% of those in the single effect cycle.

e. The cost of LPG comes out to be higher than the cost of CNG although the volume flow rate of CNG appears to be more than LPG. This is because specific volume of CNG is higher than that of the LPG.

f. The triple effect cycle is more efficient, therefore it will be more economical as compared to single and double effect cycles.

g. LPG and CNG are the best choice for operating the LiBr-H_2O absorption systems, because it can provide high temperature and are easily available at nominal costs.

REFERENCES

[1] Saghiruddin and Siddiqui, M.A., Economic Analysis and Performance Study of Three Ammonia-Absorption Cycles Using Heat Recovery Absorber, Energy Conversion and Management, No.37, pp 421-432, 1996.

[2] Saghiruddin and Siddiqui, M.A., Effect of Using a Heat Recovery Absorber on the Performance and Operating Cost of the Solar Ammonia Absorption Cycles, Journal of Solar Energy Engineering, Transactions of ASME, No.119, pp 19-23, 1997.

[3] Siddiqui, M.A., Optimum Generator Temperature in Four Absorption Cycle Using Different Sources of Energy, Energy Conversion and Management, No.24, pp 251-266, 1993.

[4] Malik, I.H. and Siddiqui, M.A., Optimization of Generator Temperatures in the Heat Operated Absorption Cycle Using Four Types of Aqueous Salt Solutions, Energy Conversion and Management, No.37, pp 433-445, 1996.

[5] Aphornratana, S. and Sriveerakul, T., Experimental Studies of a Single-Effect Absorption Refrigerator Using Aqueous Lithium–Bromide: Effect of Operating Condition to System Performance, Experimental Thermal and Fluid Science, No. 32, pp 658-669, 2007.

[6] Kaushik, S.C. and Kumar, R., Thermodynamic Study of Two Stage Vapour Absorption Refrigeration System Using NH_3 Refrigerant with Liquid Solid Absorbents, Energy Conversion and Management, No. 4, pp 427-431, 1985.

[7] Arora, A. and Kaushik, S.C ., Energy and Exergy Analysis of Single Effect and Series Flow Double Effect Water–Lithium Bromide Absorption Refrigeration Systems, International Journal of Refrigeration, 32, 6, pp 1247–1258, 2009.

[8] Marcos, J.D., Izquierdo, M. and Palacios, E., New Method for COP Optimization in Water- And Air-Cooled Single and Double Effect Libr-Water Absorption Machines, International Journal of Refrigeration, 34, 6, pp 1348–1359, 2011.

[9] Gomri Rabah and Hakimi Riad, Second law analysis of double effect vapour absorption cooler system, Energy Conversion and Management 49, pp 3343-3348, 2008.

[10] Gomri, R., Investigation of the Potential of Application of Single Effect and Multiple Effect Absorption Cooling Systems, Energy Conversion and Management, 51, pp 1629-1636, 2010.

[11] Berhane H. Gebreslassie, Marc Medrano and Dieter Boer, Exergy Analysis of Multi-Effect Water–Libr Absorption Systems: from Half to Triple Effect", Renewable Energy, 35, pp 1773-1782, 2010.

[12] Saeed Sedigh and Hamid Saffari, Thermodynamic Analysis of Triple Effect Absorption Refrigeration Systems, International Journal of Energy & Technology, 7, pp 1-8, 2012.

[13] Siddiqui, M. Altamush, Ph.D. Thesis, AMU Aligarh, 1992.

[14] Cengel, Y.A. and Boles, M.A. , Thermodynamics an Engineering Approach, Tata McGraw Hill Education Private Limited New Delhi, 2008.

[15] Kaita, Y., Thermodynamic Properties of Litium Bromide-Water Solutions at High Temperatures, International Journal of Refrigeration, 24, pp374–390, 2001.

[16] Patek, J. and Klomfar, J., Computationally Effective Formulation of The Thermodynamic Properties of Libr–H_2O Solution From 273 To 500 K Over Full Composition Range, International Journal of Refrigeration , 29, pp566–78, 2006.

[17] Gomri, R., Second Law Comparison of Single Effect and Double Effect Vapour Absorption Refrigeration Systems, Energy Conversion and Management, 50, pp 1279-1287, 2009.

[18] Holman, J. P., Heat Transfer, ninth ed., McGraw-Hill, New York, 2002.